A Model Structure for the Heterodimer apoA-I_{Milano}–apoA-II Supports Its Peculiar Susceptibility to Proteolysis

Alessandro Guerini Rocco,* Luca Mollica,† Elisabetta Gianazza,* Laura Calabresi,‡ Guido Franceschini,‡ Cesare R. Sirtori,*‡ and Ivano Eberini*

*Gruppo di Studio per la Proteomica e la Struttura delle Proteine, ‡Centro E. Grossi Paoletti, Dipartimento di Scienze Farmacologiche, Università degli Studi di Milano, Milan, Italy; and †Dulbecco Telethon Institute c/o S. Raffaele Scientific Institute, Biomolecular NMR Laboratory, Milan, Italy

ABSTRACT In this study, we propose a structure for the heterodimer between apolipoprotein A-I_{Milano} and apolipoprotein A-II (apoA-I_M–apoA-II) in a synthetic high-density lipoprotein (HDL) containing L-α-palmitoyloleoyl phosphatidylcholine. We applied bioinformatics/computational tools and procedures, such as molecular docking, molecular and essential dynamics, starting from published crystal structures for apolipoprotein A-I and apolipoprotein A-II. Structural and energetic analyses onto the simulated system showed that the molecular dynamics produced a stabilized synthetic HDL. The essential dynamic analysis showed a deviation from the starting belt structure. Our structural results were validated by limited proteolysis experiments on HDL from apoA-I_M carriers in comparison with control HDL. The high sensitivity of apoA-I_M–apoA-II to proteases was in agreement with the high root mean-square fluctuation values and the reduction in secondary structure content from molecular dynamics data. Circular dichroism on synthetic HDL containing apoA-I_M–apoA-II was consistent with the α-helix content computed on the proposed model.

INTRODUCTION

The lipoproteins are macromolecular complexes of lipid and protein, a major function of which is to transport lipids through the vascular and the extravascular body fluids. High-density lipoproteins (HDLs), the smallest and most dense lipoproteins, are involved in the reverse transport of cholesterol and exert antiatherogenic activities (1). The major protein component of HDL is apolipoprotein A-I (apoA-I) (2). The majority of HDL is spherical and contains other apolipoproteins, such as apoA-II and the C peptides, nascent HDLs are discoidal particles and contain two molecules of apoA-I (3).

Crystal structures for lipid-free apoA-I (4,5) and apoA-II (6) have been solved, but it is well known that these amphipathic proteins are structured and exert their activity solely in a lipidic environment (7). For this reason, two alternative theoretical models, based on amphipathic α-helices, have been proposed for the tertiary structure of lipid-bound apoA-I. In the picket-fence model (8), the helices run antiparallel to one another (intramolecular protein-protein interactions) and parallel to the lipid acyl chains; in the belt (or rail-fence) model (9), the helices run perpendicular to phospholipids (intermolecular protein-protein interactions). A hairpin folding has also been proposed (10), with most helices perpendicular to the phospholipid acyl chains and a random head-to-tail and head-to-head arrangement of the two apoA-I molecules. During the last years, the most credited model was the belt, but a recent article by Culot et al. (11), in which a synthetic HDL (s-HDL) was directly observed by scanning tunneling microscopy, better agrees with the picket-fence arrangement for apoA-I and other apolipoproteins. Molecular dynamics (MD) of a discoidal complex made of L-α-palmitoyloleoyl phosphatidylcholine (POPC) and a synthetic α-helical 18-mer peptide with an apolipoprotein-like charge distribution in a picket-fence arrangement has been run for 700 ps (12).

Apolipoprotein A-I_{Milano} (apoA-I_M), the first described mutant of apoA-I (13), differs from wild-type protein by the single amino-acid substitution R173C, leading to the formation of homodimers (apoA-I_M–apoA-I_M) and of heterodimers with apolipoprotein A-II (apoA-II) (apoA-I_M–apoA-II) (14). Carriers of the mutant, all heterozygous, show a very low plasma HDL-cholesterol level and a moderate hypertriglyceridemia (15), but they do not differ to any extent in the entity of carotid intima-media thickness with respect to close relatives living in the same environment and with HDL levels in the normal range (16). These observations suggest a peculiar protective effect for the apoA-I_M. The mutant apolipoprotein was selected in its homodimeric form as a drug for the treatment of atheromatous cardiovascular disease, now in clinical development (17). The apoA-I_M–apoA-I_M homodimer has both a very powerful cholesterol-removing capacity (18) and peculiar plasma kinetic characteristics, with a residence time after a single parenteral administration longer than eight days (19). In this study, we focused our attention onto the structure of the apoA-I_M–apoA-II heterodimer, which can contribute, together with the apoA-I_M–apoA-I_M homodimer, to the cardiovascular protective effects. A puzzling feature we could demonstrate in our investigation is a peculiar susceptibility to proteolysis that suggests a different and more flexible conformation than for wild-type apoA-I. To obtain a model for the apoA-I_M–apoA-II molecule we

Submitted March 27, 2006, and accepted for publication July 19, 2006.

Address reprint requests to Ivano Eberini, Tel.: 39-02-5051-8395; E-mail: ivano.eberini@unimi.it.

0006-3495/06/10/3043/07 $2.00

doi: 10.1529/biophysj.106.085886

applied bioinformatics/computational tools and procedures, starting from published crystal structures for apoA-I (4) and apoA-II (6). The model was used to build an s-HDL containing two molecules of apoA-I_M–apoA-II and 112 molecules of POPC as homogeneous phospholipid bilayer. The MD of this macromolecular complex was computed for 15 ns in explicit solvent to obtain data about the structural and dynamic properties of the antiatherogenic mutant protein apoA-I_M, in the heterodimeric form and in a lipidic environment, an essential preliminary step for understanding its biological activity.

MATERIALS AND METHODS

In vitro experiments: proteolysis

Human HDL_3 ($d = 1.125$–1.21 g/ml) were separated from plasma of fasting healthy volunteers by salt density ultracentrifugation. ApoA-I_M HDL_3 was purified from carrier plasma. Control and apoA-I_M HDL_3 (0.1 mg of protein/ml) were mixed with trypsin at the ratio of 1:50 (w/w) and incubated at 37°C. At various time intervals, aliquots were removed, SDS was added to obtain a final concentration of 4%, and samples were boiled for 2 min to terminate the reaction. The digestion products were analyzed by SDS-PAGE on 10–16% acrylamide gradient slab gels, using the Tris/HCl//Tris/tricine buffer system (20).

Purification of plasma A-I_M–A-II

HDLs ($d = 1.063$–1.21 g/ml) were isolated from apoA-I_M plasma by sequential ultracentrifugation. After delipidation, HDL apolipoproteins were solubilized in 0.1 M Tris-HC1, 0.04% EDTA, 0.01% NaN_3, pH 7.4, containing 6 M GdnHCl and applied to a Sephacryl S-300 HR column (2.6 × 300 cm) (Pharmacia Biotech, Uppsala, Sweden) equilibrated with 0.1 M Tris-HC1, 0.04% EDTA, 0.01% NaN_3, pH 7.4, containing 4 M GdnHCl. Fractions corresponding to apoA-I_M–apoA-II were concentrated and reapplied to the same column. The purity (>95%) of apoA-I_M–apoA-II preparation was confirmed by SDS-PAGE, using Coomassie protein staining. Aliquots of apoA-I_M–apoA-II were stored at −80°C in lyophilized form. Before use, apoA-I_M–apoA-II was dissolved in 20 mM phosphate buffer, pH 7.4, containing 6 M GdnHCl and extensively dialyzed against 20 mM phosphate buffer, pH 7.4.

Synthetic HDLs containing A-I_M–A-II and palmitoyloleoyl phosphatidylcholine (POPC) were prepared by the cholate dialysis technique (starting weight ratio of 2.5:1) (21). In the final preparation, all the protein was incorporated into stable s-HDL, with no lipid-free apolipoprotein remaining.

Circular dichroism (CD) spectra were recorded with a Jasco J500A spectropolarimeter at the constant temperature of 25°C (Jasco, Tokyo, Japan). Molar mean residue ellipticity (θ) was expressed in degrees × cm^2 × $dmol^{-1}$, and calculated as: $\theta = \theta_{obs} \times 115 / 10 \times l \times c$, where θ_{obs} is the observed ellipticity in degrees, 115 is the mean residue molecular weight of the proteins, l is the optical path length in cm, and c the protein concentration in g/ml. All the spectra were baseline-corrected. The α-helical content was calculated by the method of Chang et al. (22).

In silico simulations: preparation of the apoA-I_M molecule

ApoA-I_M was obtained by introducing the R173C mutation in A and B chains of wild-type apoA-I (PDB ID code: 1AV1, corresponding to amino acids 43–243 of the protein primary structure) (4) with the Biopolymer module of the Insight II suite (Accelrys, San Diego, CA). The rotamer library for cysteine was then manually explored and the most favorable energetic arrangements were selected. Another apoA-I structure (PDB ID code: 2A01) was deposited during the writing of this article (5). However, it could not have been used in our modeling procedures, because its four-helix bundle structure is not suitable to accommodate lipid molecules.

Preparation of the heterodimer apoA-I_M–apoA-II molecule

ApoA-I_M (A and B chains) was docked with apoA-II (PDB ID: 1L6L corresponding to amino acids 4–77 of the protein primary structure) (6) (J and T chains) by using ZDOCK (23) with default parameters. One-hundred solutions were generated for each A–J, A–T, and B–J chain pairs. The solutions were examined and only the complexes with a sulfur-sulfur distance < 12 Å between C^{173} in apoA-I_M and C^6 in apoA-II were accepted. The selected complexes (three for the A–J, two for the A–T, and three for the B–J pairing, third column in Table 1) were subjected to energy minimization (EM) with MOE (Chemical Computing Group, Quebec, Canada), using the CHARMM22 (24) force field, down to a root mean-square (RMS) gradient of 0.001 kcal/mol Å; a distance-dependent dielectric term ($\varepsilon = 4r$) was applied, as in Vitale et al. (25). After EM, for each chain pairing the complex with the lowest total energy was selected and submitted to a further MD of 5 ns (fourth column in Table 1). The lengths of the bonds involving the hydrogen atoms were constrained according to the SHAKE algorithm, allowing for an integration time step of 2 fs. The velocities at 300 K were randomly assigned from the Maxwell-Boltzmann distribution. Restraints were set as 2.7 Å minimum- and 3.0 Å maximum-allowed distance between the backbone oxygen atom of residue i and the backbone nitrogen atom of residue $i+4$. As reported in Vitale et al. (25), by reducing the system degrees of freedom the application of these intrahelical distance restraints is instrumental in preserving the secondary structure of α-helices. Only the A–J complex proved stable during the MD simulation (seventh column in Table 1). EM and MD were carried out with MOE on a two-processor Apple Power Mac running Apple Mac OS X version 10.3.

Preparation of the (apoA-I_M–apoA-II)$_2$ molecule

Two molecules of heterodimer apoA-I_M–apoA-II (A–J) were docked by using ZDOCK (23) with default parameters. One-hundred solutions were generated and visually examined. The only two arrangements compatible with a central phospholipid (POPC) core were energy-minimized as described above in detail.

Preparation of the s-HDL particle

The structure with the lowest energy was used for setting up the system for the molecular dynamics simulation. The preparation of the s-HDL particle

TABLE 1 Selection of the energetically favored structures for (apoA-I_M–apoA-II)$_2$ model

Dimer type	#	Total energy after EM (kcal/mol)	Total energy after MD-EM (kcal/mol)	$(Dimer)_2$ type	#	Total energy after MD-EM (kcal/mol)
A–J	87	2044.55	1944.58	$(A–J)_2$	52	3548.98
					1	3631.90
	69	2149.89				
	19	2153.70				
A–T	32	2093.19	1987.29			
	79	2257.99				
B–J	17	2095.06	2016.95			
	34	2204.38				
	2	2343.18				

required a large and equilibrated double layer of POPC: a 32 × 32 lipid-molecule equilibrated bilayer was obtained from the free-access database of bilayer structures of Peter Tieleman (http://moose.bio.ucalgary.ca/) and used to create manually a larger bilayer of 64 × 64 POPC molecules. This novel membrane structure was energy-minimized, solvated with water in a 16 × 16 × 16 nm^3 box, and minimized again; then its dynamics was simulated for 2 ns to get an equilibrated structure and to avoid any boundaries artifact. The (apoA-I_M–apoA-II)$_2$ molecule was placed into the double layer while getting as many lipid molecules as possible trapped into the hole formed by the ringlike dimer structure, in agreement with relevant experimental data about s-HDL composition (26). The lipid molecules remaining outside the hole were manually removed using the Insight II suite, running on SGI Fuel, with the aid of Stereo Graphics Crystal Eyes stereo view. The resulting s-HDL particle, containing 112 POPC molecules, was inserted in a 15 × 15 × 15 nm^3 box that was then filled with water. The system was neutralized by adding 20 Na^+ ions, minimized, and then simulated in two different steps: 1), 500 ps of position-restrained MD with an isotropic force (1000 kJ mol^{-1} nm^{-2}) applied to all protein atoms to allow for both water exit from the hydrophobic bilayer core and solvent relaxation; and 2), 15 ns of unrestrained MD. Analysis of the trajectory was started after the first nanosecond of unrestrained MD and carried out over the following 14 ns. The software package GROMACS 3.2.1 was used, both on local Apple Mac OS X-based machines for few ps trial runs and on the Avogadro Linux supercomputer at Consorzio Interuniversitario Lombardo per l'Elaborazione Automatica for the main simulation. GROMOS96 force field, modified according to Berger et al. (27) to improve lipid properties, was applied; single-point charge water model was used for the simulation of explicit solvent.

All the simulations were performed at 300 K and 1 bar with coupling constant of 0.1 ps for temperature and 1.0 ps for pressure, in both cases applying the Berendsen weak coupling algorithm. The time step for integration was set at 0.001 ps.

A twin-range cutoff of 1.0/1.7 nm for the treatment of both Coulomb and van der Waals interactions was used with neighbor list searching (updated every 10 steps).

Changes of axis orientation during MD in contiguous α-helices were monitored with the program g_helixaxis (28,29). Criteria for the selection of the structures to be monitored were: α-helix in crystal structure, motion in essential dynamics, distance from chain termini, and close proximity to next α-helix.

RESULTS AND DISCUSSION

Limited proteolysis has been applied to the study of apoA-I in different types of HDL and reconstituted lipoprotein, for structural, topological, and functional purposes. Maximal susceptibility of lipid bound apoA-I to proteolytic attack has been mapped in various experimental setups to the N-terminus (30,31), to the middle part (32–34) or to the C-terminus of the molecule (33–35). This variability hints at major plasticity of apoA-I, whose conformation appears to depend on the size of the carrier particle, mode of reconstituted HDL preparation, type of added lipid and oxidation state of methionine residues. HDL_3, obtained both from control subjects and from carriers of the Milano mutation, were digested with trypsin in a time-course setup; the pattern of the resulting proteolytic fragments is shown in Fig. 1. ApoA-II seems to be very resistant to trypsin in both the tested samples. In the apoA-I_M containing HDL_3 the susceptibility to proteolysis increases in the order: apoA-I < apoA-I_M–apoA-II < apoA-I_M–apoA-I_M.

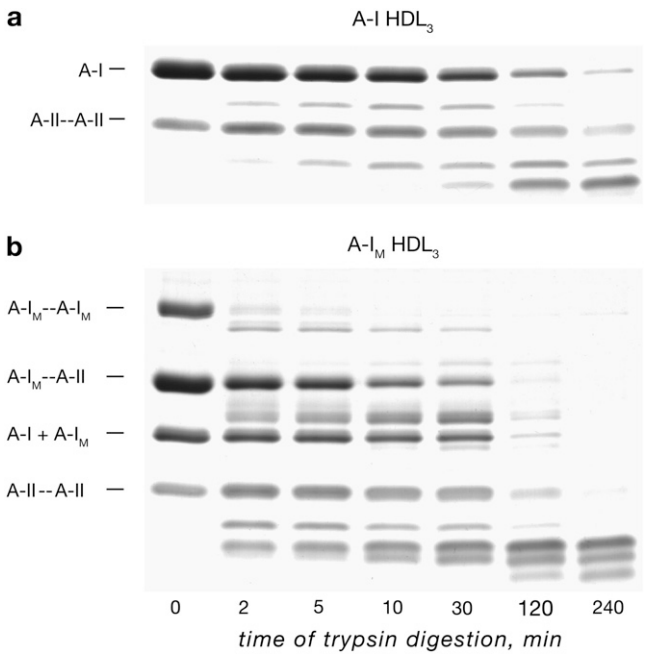

FIGURE 1 Pattern of trypsin proteolysis for apoA-I_M (*a*) and control (*b*) HDL_3, as analyzed by SDS-PAGE. HDL_3 were incubated with trypsin at 37°C (enzyme/substrate ratio, 1:50); at various times, 10 μg of protein was removed, the reaction was terminated, and the digestion products were separated by SDS-PAGE.

Proteolysis of a native protein is kinetically regulated by the differential accessibility of the various target amino acids to the enzyme. The apparent unrestrained availability to proteolytic enzymes of a larger number of target sites in homo- and heterodimeric apoA-I_M forms, with respect to wild-type apoA-I, thus suggests relevant structural differences exist between them. Availability of the recombinant protein already allowed characterization of the apoA-I_M–apoA-I_M homodimer (36). In both 7.8 and 12.5 nm s-HDL particles containing the dimer, the α-helical content of apoA-I_M is similar to that of apoA-I in small size wild-type HDL (26). Susceptibility to proteolysis of apoA-I_M–apoA-I_M is much higher than for apoA-I, cutting sites being recognized at specific positions in the middle and C-terminus (34). This observation suggests that two amino-acid stretches in α-helix structure in apoA-I are instead disordered in the homodimer, in contrast with the suggestion that apoA-I and apoA-I_M in HDL share the same belt structure (2). ApoA-I_M–apoA-II heterodimer is an abundant component of A-I_M HDLs and likely contributes to their protective effects, yet it cannot be synthesized in vitro with acceptable yields and as such is not amenable to direct characterization. Models of the molecular components peculiar to the A-I_M HDLs, the apoA-I_M–apoA-I_M homodimer, and the apoA-I_M–apoA-II heterodimer, to be compared with models of apoA-I in wild-type discoidal HDL, would help in understanding the biochemical and physiological implications of the apoA-I_M mutation. As detailed in Materials and Methods, we built in silico an s-HDL

containing two molecules of apoA-I_M–apoA-II, through the following steps:

Step 1. R173C mutation from wild-type apoA-I to apoA-I_M.
Step 2. Molecular docking between apoA-I_M and apoA-II and disulfide bonding to form the heterodimer.
Step 3. Molecular docking between two molecules of apoA-I_M–apoA-II.
Step 4. Bounding with (apoA-I_M–apoA-II)$_2$ an equilibrated bilayer of POPC to form the s-HDL.

From the published structures of apoA-I in octameric stacked form (4), chains A and B were selected as inputs because they have a shape dissimilar from one another. For apoA-II crystallized in multimeric form (6), chain J was preferred as having the curvature closest to apoA-I crystal, and chain T as having the curvature most different from apoA-I. At each Step 2–4, selection among the solutions was first on the basis of geometrical consideration (appropriate sulfur-sulfur distance in Step 2, formation of a ringlike structure in Step 3), then on the basis of energetic ranking. The potential energy of the geometrically acceptable structures after each step is charted in Table 1. Fig. 2, *a–c*, shows the result of the above docking procedures. Panel *a* is a top view of the protein chains without lipids, i.e., after Step 3 of the above sequence of procedures. Panel *b* is a top view and panel *c* is a side view of the s-HDL after Step 4, before the 15-ns MD was started. Figs. 3 and 4 (except for panel *d*) show the evolution with time of some structural and energetic parameters of the system during MD. All parameters plateau during the last stage (in no case less than the last 5 ns) of the simulation.

Gross geometrical stability is attained early in the simulation process: backbone net displacement as measured by α-carbon RMSD already quenches after 4 ns to reach a plateau after 8 ns (Fig. 3 *c*). Radius of gyration decreases down to its minimal stable value of ~4.2 nm after 8 ns (Fig. 3 *d*). This size is fully compatible with actual properties of apoA-I_M s-HDL, as known from literature data (26).

The number of interactions among protein chains (number of H-bonds in Fig. 4 *a*) increases by ~0.1-fold during the first 100 ps of simulation but then merely fluctuates; the number of salt bridges does not change with time (not shown). On the contrary, the number of interactions between protein and lipids keeps growing, to a 2.5-fold increase at 15-ns versus start of MD (Fig. 4 *b*).

Also the protein-protein interaction energies only slightly change with simulation time (not shown). On the contrary, the protein-lipid interaction energies decrease until plateau is reached at ~7 ns for short-range Coulomb (Fig. 4 *c*) and at ~9 ns for Lennard-Jones energies (Fig. 4 *d*). This evidence leads to the conclusion that the increasing number of contacts between apolipoproteins and POPC acts as the driving force for the structural reorganization of the s-HDL during the simulation. The number of amino acids in secondary structure (Fig. 3 *a*) gradually decreases by ~8%, equally distributed among the four protein chains, and approaches plateau at ~12 ns. We can conclude that the polypeptide chains are substantially less structured in the s-HDL containing (apoA-I_M–apoA-II)$_2$ than in the starting crystal structures.

For this most critical feature of the model, experimental proof was sought. A CD spectrum on an s-HDL reconstituted from plasma-purified apoA-I_M–apoA-II and POPC (Fig. 6 in Supplementary Material) measures, at 222 nm, a molar mean-residue ellipticity of −24.70 mdeg, corresponding to a helix content of 74%. A DSSP run (37) on the last minimized time frame recognizes in the model 391 aa in α-helix, 9 aa in 3-helix, 13 aa in 5-helix, for an overall helix content of 75% across a total of 548 aa in s-HDL. For the structure content in (apoA-I_M–apoA-II)$_2$, the agreement between computed and found is thus excellent.

The plot of RMSF (Fig. 3 *d*) shows two peaks of fluctuation corresponding to the C-termini of the apoA-I_M chains.

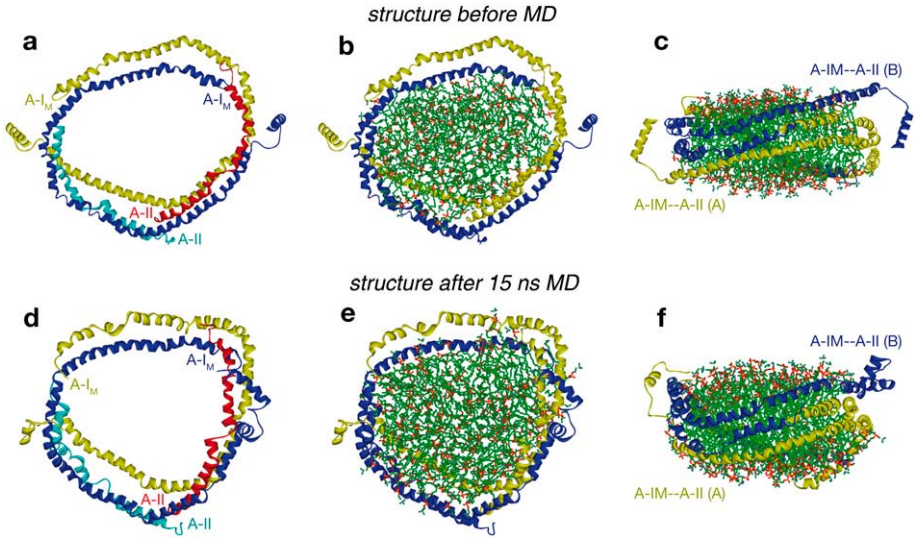

FIGURE 2 Model structure for (apoA-I_M–apoA-II)$_2$ in an s-HDL containing 112 POPC molecules. (*a–c*) Before MD; (*d–f*) after 15-ns MD. Panels *a* and *d* identify the four apolipoprotein chains (color code: *yellow* for apoA-I_M(A), *red* for apoA-II(A), *blue* for apoA-I_M(B), and *cyan* for apoA-II(B); labels near the N-termini), the remaining panels identify the two apoA-I_M–apoA-II heterodimers (color code: *yellow* for (A), *blue* for (B)). Panels *a*, *b*, *d*, and *e* are top views; *c* and *f* are side views. Protein structure is rendered as α-carbon ribbon, POPC with CPK colors (image made with Discovery Studio 1.5, Accelrys).

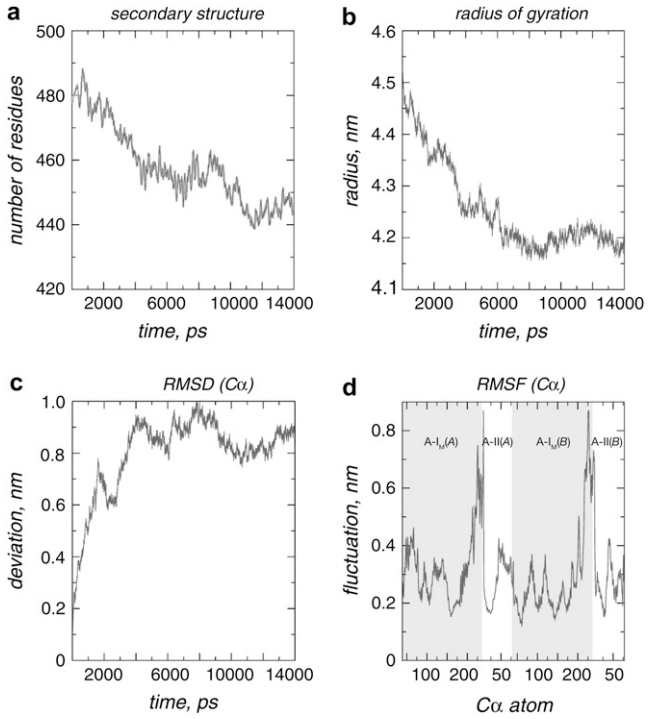

FIGURE 3 Geometrical and structural properties of (apoA-I_M–apoA-II)$_2$ s-HDL from MD run data. (*a*) Number of amino-acid residues in secondary structure; (*b*) radius of gyration; (*c*) RMSD; and (*d*) RMSF. Amino-acid numbering is according to the primary structure of apoA-I (*shaded background*) and apoA-II (*open background*). Data from the last 14 ns of simulation.

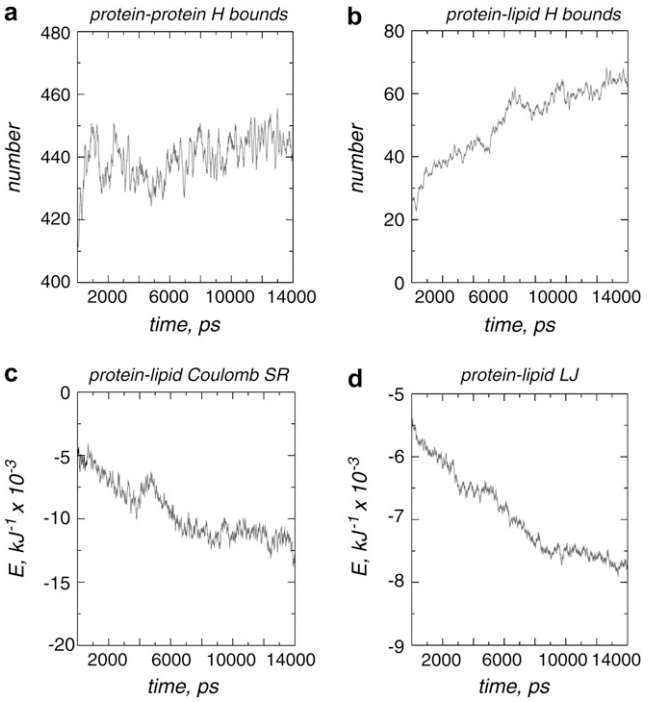

FIGURE 4 (*a*,*b*) H-bonding pattern of (apoA-I_M–apoA-II)$_2$ s-HDL from MD run data. (*a*) Number of protein-protein H-bonds; (*b*) number of protein-lipid H-bonds. Data from the last 14 ns of simulation. (*c*,*d*) Energetic properties of (apoA-I_M–apoA-II)$_2$ s-HDL from MD run data. (*c*) Coulomb short-range protein-lipid interaction energy; (*d*) Lennard-Jones protein-lipid interaction energy. Data from the last 14 ns of simulation.

The decrease in structure (Fig. 3 *a*) and the increase in protein flexibility (Fig. 3 *d*) demonstrated by MD closely agree with the finding of higher susceptibility to proteolysis seen in Fig. 1. Due to the 4 Å resolution of the crystal (4), no direct comparison of B-factor with the final structure of apoA-I_M–apoA-II is possible. The cleavage by trypsin of apoA-I_M and apoA-I_M–apoA-I_M was extensively characterized with mass spectrometry (34). Interestingly, most of the cleavage sites are located in high RMSF regions on the simulated apoA-I_M molecule; furthermore apoA-I_M has several other high RMSF regions, which can explain the proteolytic susceptibility of this mutant in its heterodimeric arrangement.

The structure of (apoA-I_M–apoA-II)$_2$-containing s-HDL after 15 ns MD is shown in Fig. 2, bottom. By pairwise comparison of Fig. 2, *d–f*, with *a–c*, some of the features already inferred from physical parameters are apparent. The C-termini of apoA-I_M(A) and (B) get closer to the lipid core while becoming less ordered; the overall structure becomes more compact. The course of the protein chains becomes tilted to a lower angle to the direction of the phospholipid acyl chains.

Our MD and ED results in Fig. 5 *a* suggest the apolipoprotein chains bend with time around four hinges. As a result, the protein increases its out-of-plane deformation, markedly deviating from a planar belt conformation. The positions of the four hinges correspond to regions in which the number of adjacent apolipoprotein chains lowers by one (at individual chain termini), allowing for higher flexibility of the system. All hinges encompass proline residues [apoA-II(A) P^{32}, apoA-II(A) P^{74}, apoA-I(B) P^{99}, and apoA-I(B) P^{143}]. Fig. 5 *c* details the changes with time of the angle between two pairs of contiguous α-helices—aa 88–98 vs. 99–120 and aa 121–142 vs. 143–164 in apoA-I_M(B)—to which the criteria for the treatment with g_helixaxis (28,29) could be applied (see under Materials and Methods). At the beginning of MD the tilt between the helices is ~45° in both pairs. This value increases to only ~50° for 88–98 vs. 99–120 but to as much as to ~70° for 121–142 vs. 143–164. The s-HDL structure packs in during the simulation time, and twisting is unevenly distributed along the apolipoprotein sequence. A very recent article (38) compared the results of 4–7 ns MD simulations of nanodiscs, similar to s-HDL, containing a fixed number of phospholipid molecules—160 DPPC per particle, according to Bayburt et al. (39) and Denisov et al. (40)—and various truncated forms of wild-type apoA-I. With the 200-amino-acid-long truncated form, extensive flexibility of the protein scaffold resulted in a severe out-of-plane deformation of apoA-I chains. With forms shorter by 11- and 22-amino acids, a planar belt structure was on the contrary observed for the protein scaffold. A planar belt structure had also been observed in the 1-ns MD

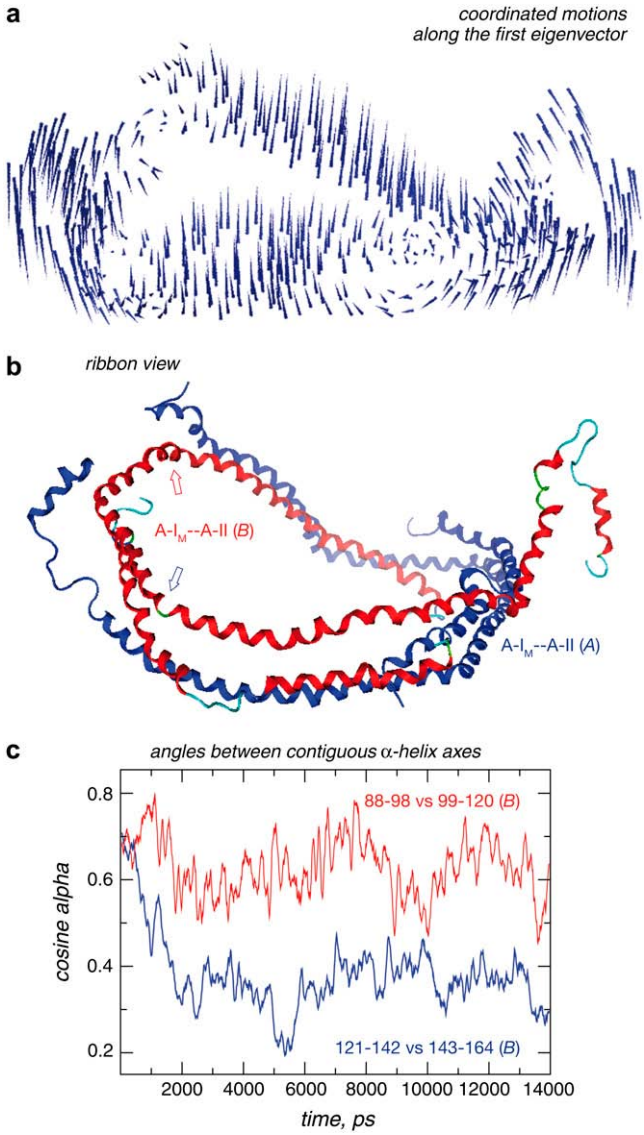

FIGURE 5 (*a*,*b*) Porcupine plot of the coordinated motions of (apoA-I_M–apoA-II)$_2$ in s-HDL during essential dynamics (ED). (*a*) The displacement of α-carbons is projected along the first eigenvector calculated by Dynamite (41). (*b*) Structure of the iso-oriented protein before MD is rendered (with MOE) in ribbon graphical mode. (*c*) Changes with time of the angles between the axes of contiguous α-helices. The tilt was computed with g_helixaxis (28,29) for α-helices to which the selection criteria detailed under Materials and Methods could be applied. Data for aa 88–98 vs. 99–120 are color-coded red; aa 121–142 vs. 143–164 are color-coded blue. The position of the relevant angles in the s-HDL structure is marked in panel *b* by arrows with the same color-code.

simulation of an s-HDL containing two 211-amino-acid-long truncated form of apoA-I and 160 molecules of POPC (2). From these data, the phospholipids/protein ratio seems crucial for the structure of s-HDL in solution.

When building the heterodimer-containing s-HDL, most POPC molecules were added to our system with an automated script, but number and position of phospholipids were then manually refined. One-hundred-and-twelve POPC molecules could be placed inside the protein ring. This phospholipids/protein ratio is very close to the experimental value (61:1) observed for s-HDL containing the 200-amino-acid-long truncated form of apoA-I (38). During our simulation, no phospholipid moved away from the s-HDL and the changes with time in lipid-lipid and protein-lipid energies (Fig. 4, *c* and *d*) confirmed a favorable rearrangement toward a more stable particle.

All of this direct and indirect evidence: stability with MD time of the in silico-generated structure, agreement between calculated and measured parameters, and conformity of experimental behavior with simulated features, are supportive to the value of the (apoA-I_M–apoA-II)$_2$ model we propose. The reported findings are suggestive that the apoA-I_M–apoA-II heterodimer, one of the major component of HDL in the carriers, may possibly act as a decoy substrate for proteases upon entering the artery wall from the circulation, thus exerting a local protection against proteolytic activity, which leads to plaque rupture. In this way, the apoA-I_M carriers, having HDL very active in cholesterol removal and with a long half-life in plasma as well as acting as high-affinity substrates for proteolytic enzymes in the arterial wall, would be provided with a highly vasoprotective lipoprotein fraction.

SUPPLEMENTARY MATERIAL

An online supplement to this article can be found by visiting BJ Online at http://www.biophysj.org.

Authors are grateful to Anna Tramontano, António M. Baptista, Tiziana Beringhelli, Franca Fraternali, Giorgio Colombo, and Annalisa Pastore for fruitful discussions and to Franco Bonomi and Stefania Iametti for assistance with CD spectra. I.E. and A.G.R. thank Claudio Arlandini for his assistance during calculations on the Consorzio Interuniversitario Lombardo per l'Elaborazione Automatica cluster.

This investigation was supported in part by grants FIRB 2001 and 2003 from Ministero dell'Istruzione, dell'Università e della Ricerca.

REFERENCES

1. Franceschini, G., P. Maderna, and C. R. Sirtori. 1991. Reverse cholesterol transport: physiology and pharmacology. *Atherosclerosis*. 88: 99–107.
2. Klon, A. E., M. K. Jones, J. P. Segrest, and S. C. Harvey. 2000. Molecular belt models for the apolipoprotein A-I Paris and Milano mutations. *Biophys. J.* 79:1679–1685.
3. Jonas, A. 1986. Reconstitution of high-density lipoproteins. *Methods Enzymol.* 128:553–582.
4. Borhani, D. W., D. P. Rogers, J. A. Engler, and C. G. Brouillette. 1997. Crystal structure of truncated human apolipoprotein A-I suggests a lipid-bound conformation. *Proc. Natl. Acad. Sci. USA*. 94:12291–12296.
5. Ajees, A. A., G. M. Anantharamaiah, V. K. Mishra, M. M. Hussain, and H. M. Murthy. 2006. Crystal structure of human apolipoprotein A-I: insights into its protective effect against cardiovascular diseases. *Proc. Natl. Acad. Sci. USA*. 103:2126–2131.
6. Kumar, M. S., M. Carson, M. M. Hussain, and H. M. Murthy. 2002. Structures of apolipoprotein A-II and a lipid-surrogate complex provide insights into apolipoprotein-lipid interactions. *Biochemistry*. 41: 11681–11691.

7. Segrest, J. P., R. L. Jackson, J. D. Morrisett, and A. M. J. Gotto. 1974. A molecular theory of lipid-protein interactions in the plasma lipoproteins. *FEBS Lett.* 38:247–258.
8. Phillips, J. C., W. Wriggers, Z. Li, A. Jonas, and K. Schulten. 1997. Predicting the structure of apolipoprotein A-I in reconstituted high-density lipoprotein disks. *Biophys. J.* 73:2337–2346.
9. Segrest, J. P., M. K. Jones, A. E. Klon, C. J. Sheldahl, M. Hellinger, H. De Loof, and S. C. Harvey. 1999. A detailed molecular belt model for apolipoprotein A-I in discoidal high density lipoprotein. *J. Biol. Chem.* 274:31755–31758.
10. Tricerri, M. A., A. K. Behling Agree, S. A. Sanchez, J. Bronski, and A. Jonas. 2001. Arrangement of apolipoprotein A-I in reconstituted high-density lipoprotein disks: an alternative model based on fluorescence resonance energy transfer experiments. *Biochemistry.* 40:5065–5074.
11. Culot, C., F. Durant, S. Lazarescu, P. A. Thiry, B. Vanloo, M. Y. Rosseneu, L. Lins, and R. Brasseur. 2004. Structural investigation of reconstituted high density lipoproteins by scanning tunneling microscopy. *Appl. Surf. Sci.* 230:151–157.
12. Sheldahl, C., and S. C. Harvey. 1999. Molecular dynamics on a model for nascent high-density lipoprotein: role of salt bridges. *Biophys. J.* 76: 1190–1198.
13. Franceschini, G., C. R. Sirtori, A. Capurso, K. H. Weisgraber, and R. W. Mahley. 1980. A-I_M Apo protein: decreased high density lipoprotein levels with significant lipoprotein modifications and without clinical atherosclerosis in an Italian family. *J. Clin. Invest.* 66: 892–900.
14. Weisgraber, K. H., S. C. Rall, Jr., T. P. Bersot, R. W. Mahley, G. Franceschini, and C. R. Sirtori. 1983. Apolipoprotein AI_{Milano}: detection of normal AI in affected subjects and evidence for a cysteine for arginine substitution in the variant AI. *J. Biol. Chem.* 258:2508–2513.
15. Franceschini, G., G. Vecchio, G. Gianfranceschi, D. Magani, and C. R. Sirtori. 1985. Apolipoprotein A-I_{Milano}: accelerated binding and dissociation from lipids of a human apolipoprotein variant. *J. Biol. Chem.* 260:16321–16325.
16. Sirtori, C. R., L. Calabresi, G. Franceschini, D. Baldassarre, M. Amato, J. Johansson, M. Salvetti, C. Monteduro, R. Zulli, M. Muiesan, and E. Agabiti-Rosei. 2001. Cardiovascular status of carriers of the apolipoprotein A-IMilano mutant: the Limone sul Garda study. *Circulation.* 103:1949–1954.
17. Nissen, S. E., T. Tsunoda, E. M. Tuzcu, P. Schoenhagen, C. J. Cooper, M. Yasin, G. M. Eaton, M. A. Lauer, W. S. Sheldon, C. L. Grines, S. Halpern, T. Crowe, J. C. Blankenship, and R. Kerensky. 2003. Effect of recombinant ApoA-I_{Milano} on coronary atherosclerosis in patients with acute coronary syndromes: a randomized controlled trial. *JAMA.* 290:2322–2324.
18. Calabresi, L., M. Canavesi, F. Bernini, and G. Franceschini. 1999. Cell cholesterol efflux to reconstituted high-density lipoproteins containing the apolipoprotein A-I_{Milano} dimer. *Biochemistry.* 38:16307–16314.
19. Roma, P., R. E. Gregg, M. S. Meng, R. Ronan, L. A. Zech, G. Franceschini, C. R. Sirtori, and H. B. Brewer, Jr. 1993. In vivo metabolism of a mutant form of apolipoprotein A-I, A-I_{Milano}, associated with familial hypo-α-lipoproteinemia. *J. Clin. Invest.* 91: 1445–1452.
20. Schägger, H., and G. von Jagow. 1987. Tricine-sodium dodecyl sulfate-polyacrylamide gel electrophoresis for the separation of proteins in the range from 1 to 100 kDa. *Anal. Biochem.* 166:368–379.
21. Matz, C. E., and A. Jonas. 1982. Micellar complexes of human apolipoprotein A-I with phosphatidylcholines and cholesterol prepared from cholate-lipid dispersions. *J. Biol. Chem.* 257:4535–4540.
22. Chang, C. T., C. S. Wu, and J. T. Yang. 1978. Circular dichroic analysis of protein conformation: inclusion of the R-turns. *Anal. Biochem.* 91:13–31.
23. Chen, R., L. Li, and Z. Weng. 2003. ZDOCK: an initial-stage protein-docking algorithm. *Proteins.* 52:80–87.
24. Mackerell, A. D., Jr., D. Bashford, M. Bellott, R. L. Dunbrack, Jr., J. D. Evanseck, M. J. Field, S. Fischer, J. Gao, H. Guo, S. Ha, D. Joseph-McCarthy, L. Kuchnir, K. Kuczera, F. T. K. Lau, C. Mattos, S. Michnick, T. Ngo, D. T. Nguyen, B. Prodhom, W. E. Reiher III, B. Roux, M. Schlenkrich, J. C. Smith, R. Stote, J. Straub, M. Watanabe, J. Wiorkiewicz-Kuczera, D. Yin, and M. Karplus. 1998. All-atom empirical potential for molecular modeling and dynamics studies of proteins. *J. Phys. Chem. B.* 102:3586–3613.
25. Vitale, R. M., C. Pedone, P. G. De Benedetti, and F. Fanelli. 2004. Structural features of the inactive and active states of the melanin-concentrating hormone receptors: insights from molecular simulations. *Proteins.* 56:430–448.
26. Calabresi, L., G. Vecchio, F. Frigerio, L. Vavassori, C. R. Sirtori, and G. Franceschini. 1997. Reconstituted high-density lipoproteins with a disulfide-linked apolipoprotein A-I dimer: evidence for restricted particle size heterogeneity. *Biochemistry.* 36:12428–12433.
27. Berger, O., O. Edholm, and F. Jahnig. 1997. Molecular dynamics simulations of a fluid bilayer of dipalmitoylphosphatidylcholine at full hydration, constant pressure, and constant temperature. *Biophys. J.* 72: 2002–2013.
28. Christopher, J. A., R. Swanson, and T. O. Baldwin. 1996. Algorithms for finding the axis of a helix: fast rotational and parametric least-squares methods. *Comput. Chem.* 20:339–345.
29. Lensink, M. F., B. Christiaens, J. Vandekerckhove, A. Prochiantz, and M. Rosseneu. 2005. Penetratin-membrane association: W48/R52/W56 shield the peptide from the aqueous phase. *Biophys. J.* 88:939–952.
30. Lins, L., S. Piron, K. Conrath, B. Vanloo, R. Brasseur, M. Rosseneu, J. Baert, and J.-M. Rusysschaert. 1993. Enzymatic hydrolysis of reconstituted dimyristoylphosphatidylcholine-apo A-I complexes. *Biochim. Biophys. Acta.* 1151:137–142.
31. Roberts, L. M., M. J. Ray, T.-W. Shih, E. Hayden, M. M. Reader, and C. G. Brouillette. 1997. Structural analysis of apolipoprotein A-I: limited proteolysis of methionine-reduced and -oxidized lipid-free and lipid-bound human apo A-I. *Biochemistry.* 36:7615–7624.
32. Kunitake, S. T., G. C. Chen, S. F. Kung, J. W. Schilling, D. A. Hardman, and J. P. Kane. 1990. Pre-β high density lipoprotein: unique disposition of apolipoprotein A-I increases susceptibility to proteolysis. *Arteriosclerosis.* 10:25–30.
33. Dalton, M. B., and J. B. Swaney. 1993. Structural and functional domains of apolipoprotein A-I within high density lipoproteins. *J. Biol. Chem.* 268:19274–19283.
34. Calabresi, L., G. Tedeschi, C. Treu, S. Ronchi, D. Galbiati, S. Airoldi, C. R. Sirtori, Y. Marcel, and G. Franceschini. 2001. Limited proteolysis of a disulfide-linked apoA-I dimer in reconstituted HDL. *J. Lipid Res.* 42:935–942.
35. Ji, Y., and A. Jonas. 1995. Properties of an N-terminal proteolytic fragment of apolipoprotein A-I in solution and in reconstituted high density lipoproteins. *J. Biol. Chem.* 270:11290–11297.
36. Calabresi, L., G. Vecchio, R. Longhi, E. Gianazza, G. Palm, H. Wadensten, A. Hammarström, A. Olsson, A. Karlström, T. Sejlitz, H. Ageland, C. R. Sirtori, and G. Franceschini. 1994. Molecular characterization of native and recombinant apolipoprotein A-I_{Milano} dimer: the introduction of an interchain disulfide bridge remarkably alters the physicochemical properties of apolipoprotein A-I. *J. Biol. Chem.* 269:32168–32174.
37. Kabsch, W., and C. Sander. 1983. Dictionary of protein secondary structure: pattern recognition of hydrogen-bonded and geometrical features. *Biopolymers.* 22:2577–2637.
38. Shih, A. Y., I. G. Denisov, J. C. Phillips, S. G. Sligar, and K. Schulten. 2005. Molecular dynamics simulations of discoidal bilayers assembled from truncated human lipoproteins. *Biophys. J.* 88:548–556.
39. Bayburt, T. H., Y. V. Grinkova, and S. G. Sligar. 2002. Self-assembly of discoidal phospholipid bilayer nanoparticles with membrane scaffold proteins. *Nano Lett.* 2:853–856.
40. Denisov, I. G., Y. V. Grinkova, A. A. Lazarides, and S. G. Sligar. 2004. Directed self-assembly of monodisperse phospholipid bilayer nanodiscs with controlled size. *J. Am. Chem. Soc.* 126:3477–3487.
41. Barrett, C. P., B. A. Hall, and M. E. Noble. 2004. Dynamite: a simple way to gain insight into protein motions. *Acta Crystallogr. D Biol. Crystallogr.* 60:2280–2287.